Development of New Hybrid VOCs Treatment Process Using Activated Carbon and Electrically Heated Alumite Catalyst

Toshio Yᴀᴍᴀɢᴜᴄʜɪ, Kazuya Aᴏᴋɪ, Makoto Sᴀᴋᴜʀᴀɪ and Hideo Kᴀᴍᴇʏᴀᴍᴀ

Department of Chemical Engineering, Tokyo University of Agriculture and Technology, 2-24-16 Nakacho, Koganei-shi, Tokyo 184-8588, Japan

The purpose of this research is the development of a hybrid volatile organic compounds (VOCs) treatment process, which consists of adsorptive separation and catalytic oxidation. This process greatly reduces energy consumption compared with conventional thermal or catalytic combustion processes. Low concentrations of VOCs in polluted air are initially separated and concentrated into a small stream in the adsorptive step, and the concentrated VOCs are oxidized on an electrically heated alumite catalyst. Numerical system evaluation was carried out to estimate the effect of the concentration of VOCs in the air on the material and energy balances. Experimental and theoretical studies were performed on the adsorption of toluene in nitrogen gas, and desorption and concentration by hot nitrogen purging, in fixed-beds charged with activated carbon. A linear driving force mass-transfer model with an averaged overall mass-transfer coefficient was found to provide an acceptable fit to the measured desorption data. The experimental and modeling results were used to assess the influence of the purge gas flow rate and regeneration temperature on the bed length and cyclic steady-state convergence times using cyclic dynamic simulation of thermal swing adsorption. The evaluation results showed that a large amount of energy could be saved, and the unit cost lowered, by combining the adsorption step with electrically heated catalytic oxidation in the treatment of gases with low VOCs concentrations.

Introduction

Suspended particulate matter (SPM) and photochemical oxidants are among the most serious air pollutants, and are suspected of having adverse effects on human health. Action to deal with this problem is therefore urgently needed. Volatile organic compounds (VOCs) are believed to be one of the substances that generate SPM and photochemical oxidants. The target levels for VOC emissions to the atmosphere set by governments have been significantly reduced.

Large VOC-emitting facilities have obligations to minimize VOC emissions, and most large facilities have already taken appropriate measures. However, most small and medium-sized facilities have not done so, because VOC treatment facilities are relatively large scale and expensive, and running costs are incurred. An efficient and economical VOC treatment technology is needed for low concentrations of VOCs in polluted air, which has been treated by thermal combustion or catalytic oxidation adding supplementary fuel or heat.

In a previous paper (Ueno *et al.*, 2010), we reported a process that enables us to reduce energy consumption in the treatment of polluted air with low VOCs contents and to reduce equipment costs for small and medium-sized facilities by combining catalytic combustion with adsorption

technology.

Figure 1 shows a schematic process flow diagram of a new VOCs treatment process (Yamaguchi *et al.*, 2011). One of the main features of this process is enrichment of low-concentration VOCs gases in polluted air prior to catalytic combustion. By concentrating the VOCs gases into a small air stream, the adiabatic temperature rise for VOCs combustion increases and the amount of exhaust gas decreases. It is then possible to sustain catalytic combustion without supplementary heating or fuel, or with reduced amounts of heating or fuel. Furthermore, the heat of exhaust gas emitted to the atmosphere is reduced. The catalytic combustion heat is recovered and used for preheating the feed gas to the catalytic oxidizer and desorption air fed to the adsorber. When surplus heat remains after preheating and heating, it may be
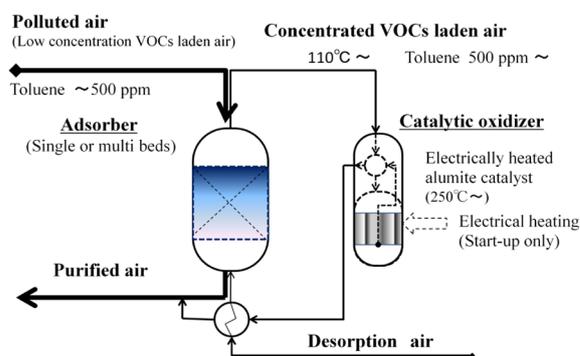
Fig. 1 Schematic process flow diagram of new VOCs treatment process

used for other purposes.

Another main feature is the installation of an electrically heated alumite catalytic oxidizer. The alumite catalyst can be rapidly heated electrically because it is a monolith of an electric heater and catalyst. The flowing VOCs gas contacts the heated catalyst directly. The electrically heated alumite catalyst is advantageous for rapid responses in temperature control of the catalyst and gas flow (Guo *et al.*, 2003; Kameyama, 2005).

Various papers have reported parametric analysis or studies of regeneration in thermal swing adsorption (TSA), including optimization of the purge gas quantity and the energy required for regeneration (Basmadjian *et al.*, 1975; Kumar and Dissinger, 1986; Huang and Fair, 1988; Schork and Fair, 1988; Huang *et al.*, 1993; Hwang *et al.*, 1997; Yun *et al.*, 2000), cyclic simulation of the TSA system (Ko *et al.*, 2002a, 2002b; Ruthven, 1984), and empirical experimental analysis of the honeycomb rotor concentrator (Lin and Chang, 2009; Mitsuma *et al.*, 1998). However, there have been few numerical studies of the concentration behavior of low-concentration VOCs gases in air by lowering the purge flow rate in fixed beds packed with granular or cylindrical adsorbents.

In this study, experimental and parametric analyses of desorption and concentration were performed to investigate the concentration behavior of low-concentration VOCs in air by lowering the purge gas flow rate, through laboratory experimentation and computer modeling.

For a commercial-scale unit for this developing new process, simplified mathematical modeling was used to analyze the effects of the concentration ratio and the exhaust gas temperature on the system energy balance and supplementary or surplus heat, which were estimated for VOCs catalytic combustion.

Further experimental and modeling results were used to assess the influence of the concentration behavior on the adsorbent volume required, and the cyclic steady-state (CSS) convergence times for various regeneration temperatures using cyclic simulation of the CSS, in which the transient process conditions in the cycle remain the same in all subsequent cycles.

1. Mathematical Modeling

1.1 Adsorption and desorption

A mathematical model for fixed-bed adsorption and desorption was developed to analyze and simulate the column dynamics of the temperatures and concentrations for adsorption and thermal regeneration. The model developed is based on non-equilibrium, non-isothermal, and non-adiabatic conditions. Gas–solid, gas–column, and column–atmosphere heat-transfer resistances are considered. A linear driving force (LDF) expression with an averaged overall mass-transfer coefficient represents the gas–solid mass-transfer rate. The assumptions made in developing the model equations are as follows.
1) The ideal gas law applies.

2) The velocity of the gas is constant throughout the bed.
3) The pressure gradient across the bed is neglected.
4) The radial temperature, concentrations, and velocity gradients within the bed are negligible.
5) The mass-transfer rate is represented by an LDF expression.
6) The adsorption equilibrium is represented by a Langmuir isotherm.
7) The amount of carrier gas adsorbed is negligible.
8) The physical properties of the gas phase are the same as those of the feed gas.
9) The physical properties of the adsorbent and the column wall are assumed to be constant.

Application of the above assumptions to the material balance of the gas phase through a packed bed gives Eq. (1).

$$\varepsilon \frac{\partial C}{\partial t} + u \frac{\partial C}{\partial z} + \rho_s \frac{\partial q}{\partial t} = 0 \tag{1}$$

The energy balance is non-isothermal, with no conduction conditions.

The energy balance around the gas phase includes heat transfer to the solid phase and to the column wall.

$$c_{vg} u \rho_g \frac{\partial T_g}{\partial z} + \varepsilon c_{vg} \rho_g \frac{\partial T_g}{\partial t} + P \frac{\partial u}{\partial z} h_s a_P (T_g - T_s)$$
$$+ \frac{4h_w}{D_B}(T_g - T_w) = 0 \tag{2}$$

The energy balance around the solid phase includes the heat generated by adsorption of the adsorbate.

$$\rho_s c_{ps} \frac{\partial T_s}{\partial t} + \rho_s \sum_{i=1}^{n}(c_{pai} w_i) \frac{\partial T_s}{\partial t}$$
$$+ \rho_s \sum_{i=1}^{n}\left(\Delta H_{adi} \frac{\partial q_i}{\partial t}\right) - h_s a_P(T_g - T_s) = 0 \tag{3}$$

Heat transfer from the gas phase and to the atmosphere is included in the energy balance around the column wall.

$$\rho_w c_{pw} \frac{\partial T_w}{\partial t} - h_w \frac{4D_B}{(D_B + W_T)^2 - D_B^2}(T_g - T_w)$$
$$+ h_{amb} \frac{4(D_B + W_T)^2}{(D_B + W_T)^2 - D_B^2}(T_w - T_{amb}) = 0 \tag{4}$$

In the above equations, the mechanisms of heat transfer are expressed as linear functions of the overall driving forces. Similarly, the mass-transfer rates of the gas and solid phases can be expressed by the following LDF model given as Eq. (5).

$$\rho_s \frac{\partial q}{\partial t} = \overline{K_F a_V}(c - c^*) \tag{5}$$

A temperature-dependent extended-Langmuir isotherm is used to represent the gas–solid equilibrium isotherm.

$$q = \frac{IP_1 e^{IP_2/T_s} c}{1 + IP_3 e^{IP_4/T_s} c} \tag{6}$$

Besides the above equation, various temperature-depen-

dent extended-Langmuir models are suggested and used based on the concept that the monolayer coverage decreases with increasing temperature because of the increasing molecular area (Malek and Farook, 1996). In this simulation, we used the ASPEN ADSORPTION software package (Aspen Technology, Inc., 2006), using the LDF model.

1.2 System energy balance

Figure 2 shows a schematic block flow diagram of the new VOCs treatment process, which was used for system evaluation. This process involves two main units: namely a catalytic oxidizer and a TSA unit. This system can be used under continuous and intermittent operation. The TSA unit is operated in a cyclic manner for removing VOCs in polluted air using granular or cylindrical activated carbon. VOCs adsorbed onto the activated carbon can be desorbed by hot air and concentrated using a small amount of air for desorption. The concentrated VOCs gas is preheated by hot catalytic oxidizer exhaust gas to initiate combustion. When sufficient heat cannot be obtained for initiating combustion, supplementary heating can be supplied from an outside heat source.

Combustion of the VOCs gas proceeds adiabatically in the catalyst. When supplementary heat is needed to sustain catalytic combustion, it is supplied by an auxiliary heater. The temperature of the catalytic oxidizer exhaust gas increases as the catalytic combustion proceeds. High-temperature exhaust gas is used to preheat the feed gas to the catalytic oxidizer. The exhaust gas from the preheater is used for heating the air for desorption of the activated carbon in the fixed bed. When the combustion exhaust gas has sufficient heat for recovery, the surplus heat can be used for other purposes. The system energy balance was studied for a commercial-scale new hybrid VOCs treatment unit for the purpose of system evaluation. The following assumptions were made for system evaluation.

1) Polluted air to be treated is fed at a constant flow rate, and the VOC in the gas to be treated is toluene. Complete combustion is achieved in the catalytic oxidizer.
2) The VOCs treatment unit is operated continuously.
3) The VOCs concentration ratio, α, is controlled by the concentration ratio of the polluted air feed rate to the purge gas flow rate, and defined as F_{pair}/F_{air}.
4) A commercial activated carbon and catalyst are used as the adsorber and oxidizer, respectively.
5) Blowers are provided for feeding the polluted air and desorption air.
6) Heat loss and adsorption and desorption heats are not considered.
7) Heat exchange between adsorbers in the thermal swing operation is ignored.

The supplementary heat or surplus heat required to sustain catalytic combustion can be estimated for the new VOCs treatment as follows.

$$H_{air} + H_{VOC} = H_{out}(T) - Q \tag{7}$$
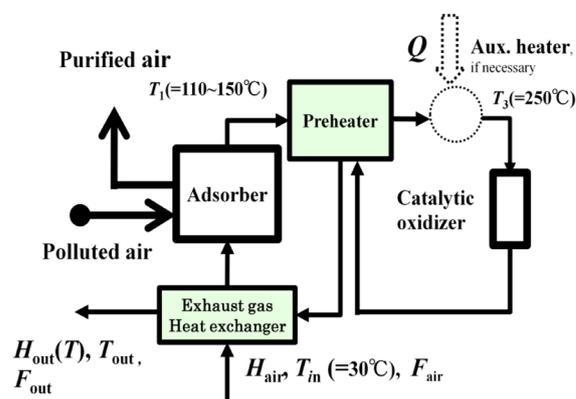
Fig. 2 Schematic block flow diagram of new VOCs treatment process for system evaluation

$$Q = (H_{out}(T_{out}) - H_{air}(T_{air}) - H_{VOC}) \times 10^{-3} \tag{8}$$

$$= (F_{out} C_{pgT}(T_{out})(T_{out} - 25) - F_{air} C_{pgT}(T_{air})$$
$$\times (T_{air} - 25) - H_{VOC}) \times 10^{-3} \tag{9}$$

2. Experimental Apparatus and Results

2.1 Materials and Methods

The experiments were performed using the dynamic flow method (Chuang *et al.*, 2003) with a fixed bed packed with granular activated carbon. Toluene was used as the VOC adsorbate to study the adsorption and regeneration on activated carbon. The experimental apparatus is shown in **Figure 3**.

Commercially available GG10/20 granular activated carbon (Kuraray Chemical Co., Ltd.) was used. The granular activated carbon was heated to 110°C in a nitrogen atmosphere to remove moisture and any adsorbed gases. The properties of this activated carbon are shown in **Table 1**.

Toluene was vaporized in a container with diffusion tubes. High-purity nitrogen was used as the carrier gas to dilute the adsorbate to the desired concentration. Some of the nitrogen gas fed to the adsorption column was bypassed into the container as a carrier for the vaporized toluene. The concentration of toluene in the carrier gas was controlled by the number of diffusion tubes and the vaporization temperature, as well as by the carrier gas flow rate. The generated VOC gas was returned to the nitrogen gas stream and the mixed gas was introduced into the adsorption column. The concentration of toluene in the feed gas to the adsorption column was kept constant.

After completing the toluene adsorption run in the activated carbon bed, desorption and concentration runs were performed by heating the column bed using a flow of hot nitrogen gas.

The temperatures of the adsorption column feed gas and the adsorption column and bed were controlled by a heated thermal oil bath, using a temperature controller. The temperature of the thermal oil can be controlled in the range 30 to 180°C.

During the experimental runs, the outlet concentration
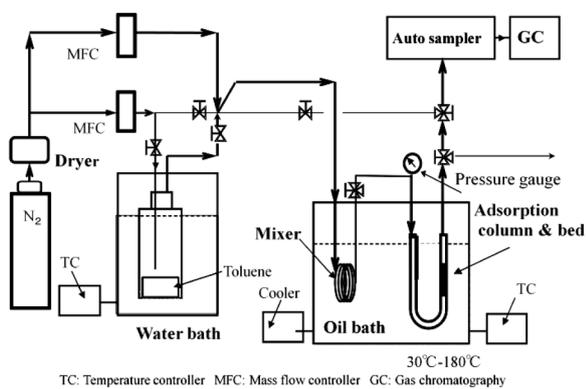
Fig. 3 Schematic block flow diagram of experimental apparatus

Material:	Glass	
Size:	Outer diameter	12 mm
	Inner diameter	8 mm
	Thickness	2 mm
	Height	244 mm

Table 1 Properties and packing characteristics of Kuraray Chemical GG10/20

Raw material	Coconut shell
Shape	Granular
Bed density [kg·m⁻³]	500–550
Bed void fraction	0.40
Particle size	0.75–1.7 mmϕ (1–1.4 mmϕ (>70%))

of the gas stream was monitored at constant time intervals (5 min) by a gas chromatograph with a flame ionization detector, automatic six-port injection valves, and a digital timer. These results were used to generate adsorption breakthrough and desorption curves.

2.2 Isotherms and adsorption rate

The experimental and modeling results for the adsorption run have been reported by the authors in a previous paper (Yamaguchi *et al.*, 2013).

The amount of adsorbed VOC vapor in equilibrium with the initial concentration was determined by graphical integration of the experimental breakthrough curve.

Figure 4 shows the temperature-dependent Langmuir adsorption isotherm that was produced based on the experimental data. The temperature-dependent form of the Langmuir isotherm equation described the adsorption data well.

Based on the mass transfer zone (MTZ) method and applying a constant pattern flow, the MTZ and overall mass-transfer coefficient were estimated. Constant pattern flows were established using column bed length of above approximately 0.01 m, as presented in our previous paper (Yamaguchi *et al.*, 2013).

Figure 5 shows the averaged overall mass-transfer coefficients obtained by the MTZ and curve-fitting methods. The obtained mass-transfer coefficients were used for simulations using the LDF model. The experimental breakthrough curves were compared with the theoretical curves obtained
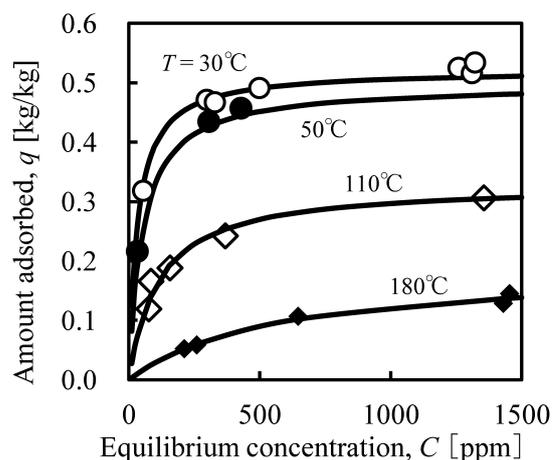
Fig. 4 Toluene isothermal data on G10/20 activated carbon
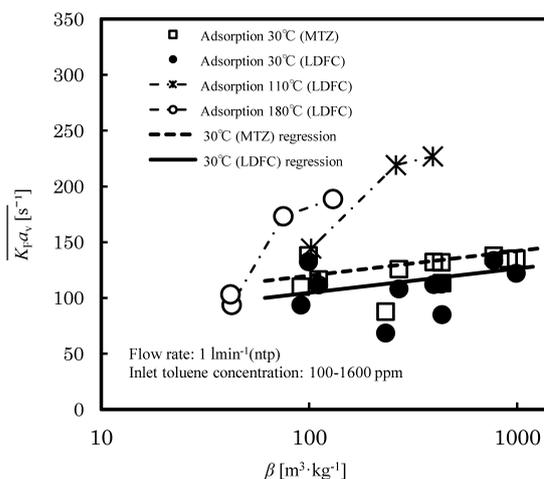
Fig. 5 Dependence of averaged overall mass-transfer coefficient, $\overline{K_F a_V}$, on β

from the mathematical model. The LDF model using mass-transfer coefficients obtained by the MTZ method gave a good prediction of the experimental results.

2.3 Desorption tests and analysis results

To study the effects of purge gas flow rate and regeneration temperature on the concentration profile of the desorbed gas in the regeneration step, experimental runs for the adsorption and regeneration steps were performed. The experimental regeneration runs were continuations of the previous adsorption runs, to complete the cycle. The feed gas flow rate was 1 L·min⁻¹ for the adsorption step. The toluene inlet concentration for the adsorption runs was in the range from about 400 to 600 ppm. The temperature of the inlet gas for the adsorption runs was 30°C. The temperature of the adsorption column bed was in the range up to 180°C, achieved using heated thermal oil, for the desorption tests. Three regeneration temperatures, 120, 150, and 180°C for the oil bath were chosen. Thermal oil was heated at the rate of approximate 2°C/min from 30°C to respective regeneration temperatures. The concentration ratio, which was de-
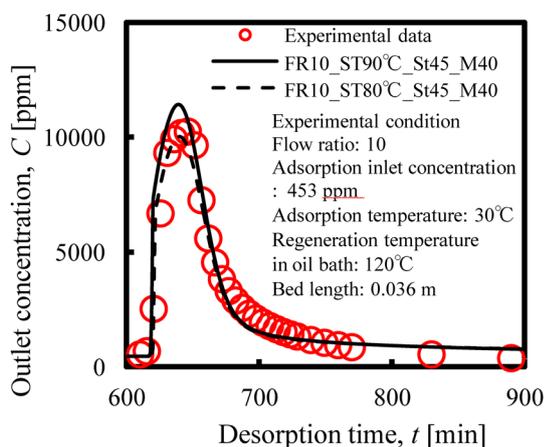
Fig. 6 Enrichment of toluene at desorption step: Comparison of experimental data and simulation results (1)

Fig. 7 Enrichment of toluene at desorption step: Comparison of experimental data and simulation results (2)


Fig. 8 Enrichment of toluene at desorption step: Comparison of experimental data and simulation results (3)

fined as the ratio of the feed gas flow rate to the hot nitrogen purge gas flow rate, was varied in the range 1–10.

In the initial period of the regeneration step, the temperatures of the adsorption column feed gas and the adsorption column and bed were raised to the target regeneration temperature by the thermal oil bath, the temperature of which was controlled by an electric heater with a temperature controller.

A time lag in the temperature rise between the thermal oil in the bath and the adsorption column inlet gas occurred when the adsorption column and bed and adsorption column feed gas were heated in the thermal oil bath. **Figures 6–8** show the fitting results of the simulation for the experimental data of desorption concentration profiles; fitting was performed at various oil bath temperatures from 120 to 180°C for a concentration ratio of 10.

An assumption was made in simulating the desorption concentration profile. The inlet gas temperature was assumed to rise along the sigmoid curve to a certain temperature and thereafter to be slowly asymptotic to the set temperature of the thermal oil.

The experimental data of the desorption concentration profile were fitted by simulation as a function of a target temperature and a rate of temperature rise for the sigmoid curve for the initial regeneration temperature rise. The averaged mass transfer coefficient for desorption was assumed, according to Figure 5, which was reported by the authors in a previous paper, taking the r–ζ method (Kawazoe, 1965; Yamaguchi *et al.*, 2013) into consideration. The gas–solid heat transfer coefficient was estimated using the following Plandl number correlation.

$$h_{\mathrm{s}} = j C_{\mathrm{pg}} u \rho_{\mathrm{g}} Pr^{-2/3} \tag{10}$$

$$\text{If } Re_{\mathrm{p}} < 190 \text{ then } j = 1.66 Re_{\mathrm{p}}^{-0.51} \tag{11}$$

$$\text{Otherwise } j = 0.983 Re_{\mathrm{p}}^{-0.41} \tag{12}$$

The flow ratio, target temperature and period for the sigmoid curve and averaged mass transfer coefficient used in
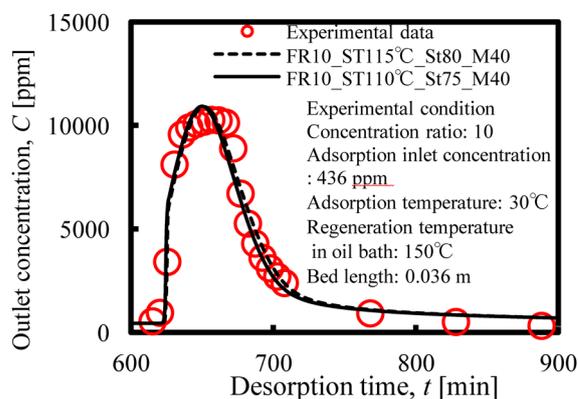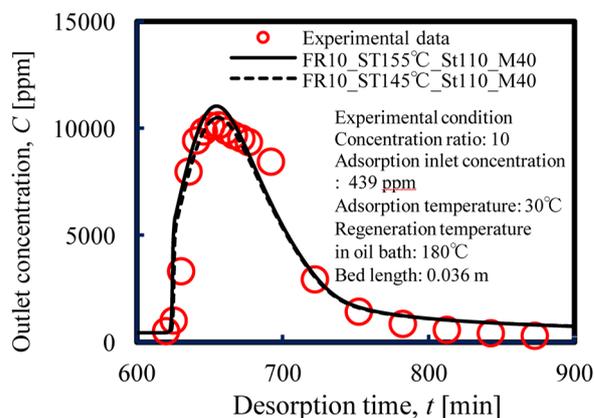
the simulation are indicated respectively in the figures.

The mathematical model was slightly modified for simulation to meet the heating mechanism of the adsorber column in the oil bath. Heat transfer from the thermal oil to wall of the adsorber column was ignored.

The calculation results indicated an acceptable fit to the measured data using the temperature-dependent extended-Langmuir equilibrium equation. Isotherm constants for Eq. (6) are as follows.

$$IP_1 = 0.2285 \text{ kmol kg}^{-1}, \quad IP_2 = 3020 \text{ K}$$

$$IP_3 = 520 \text{ kmol m}^{-3}, \quad IP_4 = 2230 \text{ K}$$

The experiments and simulation results shown in Figures 6–8 indicate that maximum concentration and concentration profile depend on the rate of temperature rise of adsorbent and equilibrium of adsorbate rather than the regeneration temperature of adsorbent.

Figure 9 shows fitting of the simulation results with the experimental data for a concentration ratio of 5, which was performed at a regeneration temperature of 180°C in the oil bath, to assess the effect of the concentration ratio on the desorption concentration profile. These calculation results also indicated an acceptable fit to the measured data using the temperature-dependent extended-Langmuir equilibrium
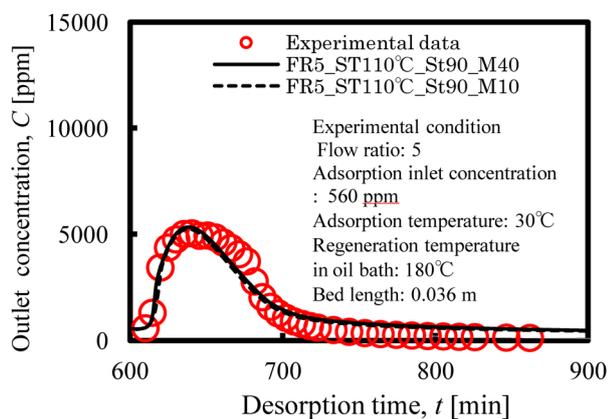
Fig. 9 Enrichment of toluene at desorption step: Comparison of experimental data and simulation results (4)

Table 2 Criteria for system evaluation

Flow rate of polluted air: $6000\,\mathrm{Nm^3\,h^{-1}}$
VOCs content in polluted air: 100, 300 ppm
Temperature of polluted air: 30°C
Temperature of desorption air and cooling gas: 30°C
Desorption feed gas temperature: 110–150°C
Catalytic oxidizer inlet gas temperature: 250°C

equation. A comparison of the experimental desorption concentration profiles at concentration ratios of 5 and 10 shows that the maximum concentration of the roll-up is greately affected by the flow ratio or concentration ratio.

3. Evaluation of New VOCs Treatment Process

3.1 Criteria for system evaluation

System evaluation of the commercial-scale new hybrid VOCs treatment unit was performed to investigate the effect of concentrating the VOCs in polluted air. The system configuration and mathematical modeling for this system are described in Section 1.2. The evaluation criteria are shown in **Table 2**.

3.2 Evaluation results

Figures 10(a) and **(b)** show the estimation results for supplementary heat or excess heat required for self-sustaining catalytic combustion. The supplementary heat or surplus heat is shown as a function of the concentration ratio and exhaust gas temperature for inlet toluene concentrations of 300 ppm and 100 ppm. The required concentration ratio is highly dependent on the temperature and flow rate of the exhaust gas to the atmosphere. As the exhaust gas temperature increases, or when the inlet toluene concentration in the polluted air is low, higher concentration ratios are needed for self-sustaining catalytic combustion.

Figure 11 shows the supplementary heat or surplus heat as a function of the concentration ratio at a constant exhaust gas temperature of 150°C and inlet toluene concentrations of 300 ppm or 100 ppm, respectively. The supplementary
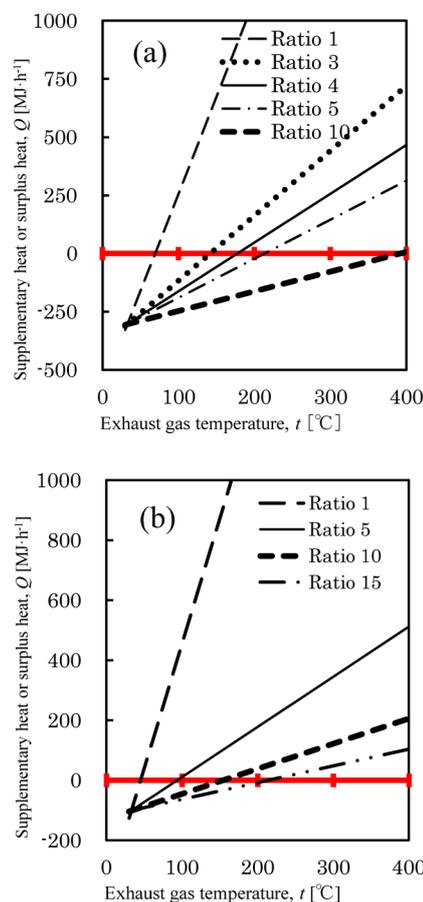

Fig. 10 Dependence of supplementary heat or surplus heat on concentration ratio of VOCs gas and exhaust gas temperature (a) toluene concentration in polluted air: 300 ppm (b) toluene concentration in polluted air: 100 ppm
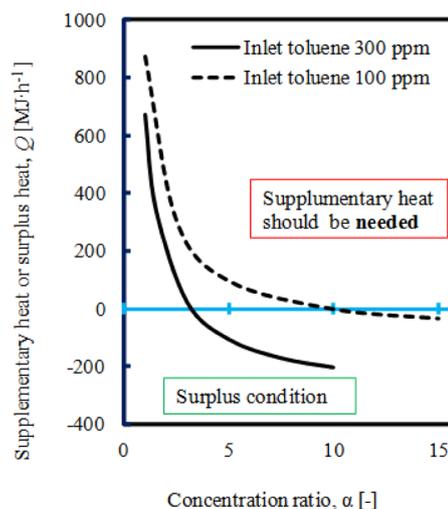

Fig. 11 Analysis of system energy balance: Effect of concentration ratio on thermal efficiency

heat or surplus heat curves rapidly decrease in the low-concentration-ratio range as the concentration ratio increases. As the concentration ratio increases further, the curves for supplementary heat or surplus heat slowly approach an as-

Table 3 Cycle sequence table for TSA

Regeneration temperature [°C]	110	130	150
Adsorption [min]	360	360	360
Heating [min]	100	120	135
Regeneration [min]	210	190	175
Cooling [min]	50	50	50

ymptotic value, namely the combustion heat of the VOCs.

As the VOCs concentration ratio increases, the size of the catalytic oxidizer and related equipment, and the electric power for desorption by the air fan decrease.

The electrically heated alumite catalyst makes it easy to respond to fluctuations in temperature and VOCs concentration, and makes it possible to reduce the system size since a combustion heater is not needed.

3.3　Simulation of cyclic steady-state operation of TSA

To enrich the VOCs concentration in the feed polluted gas, it is necessary to lower the ratio of the purge flow rate to the feed flow rate. As the purge flow rate is lowered, the desorption ability decreases because desorption is seldom carried to completion at the end of a desorption cycle. A number of cycles are required to approach the CSS condition, in which the concentration at all positions at any time in the cycle remains the same in all subsequent cycles.

A parametric study of the influence of the purge flow rate or the concentration ratio and regeneration temperature on the required bed length and CSS convergence time was performed, based on the experimental and modeling results.

To assess the effect of the VOCs concentration ratio on the adsorber design, a simulation study was performed based on the above described mathematical modeling shown in Section 1.1 "Adsorption and desorption" with the above evaluation criteria using the experimental analysis data. The additional assumptions made for the calculation were as follows.

1) The energy balance was ignored to simplify the numerical studies.
2) The granular activated carbon used in the laboratory experiments was used in this study.
3) The cycle time of TSA was assumed according to the regeneration temperature as shown in **Table 3**.
4) The temperature of polluted, desorption and cooling air was assumed to be 30°C.
5) The adsorbent was heated to various target temperatures, according to a sigmoid curve, prior to regeneration.

The simulation results are shown in **Figure 12(a)–(c)**. CSS cycles were obtained by simulation for a VOCs concentration ratio of 5 for 300 ppm of toluene in polluted air.

Figure 13 shows the influence of the concentration ratio and regeneration temperature on the bed length of the toluene loading. As the purge flow rate is lowered to increase the concentration ratio, the front edge of the adsorbent loading profile proceeds towards the bed outlet in the CSS for a two-bed TSA system. As the regeneration temperature decreases,
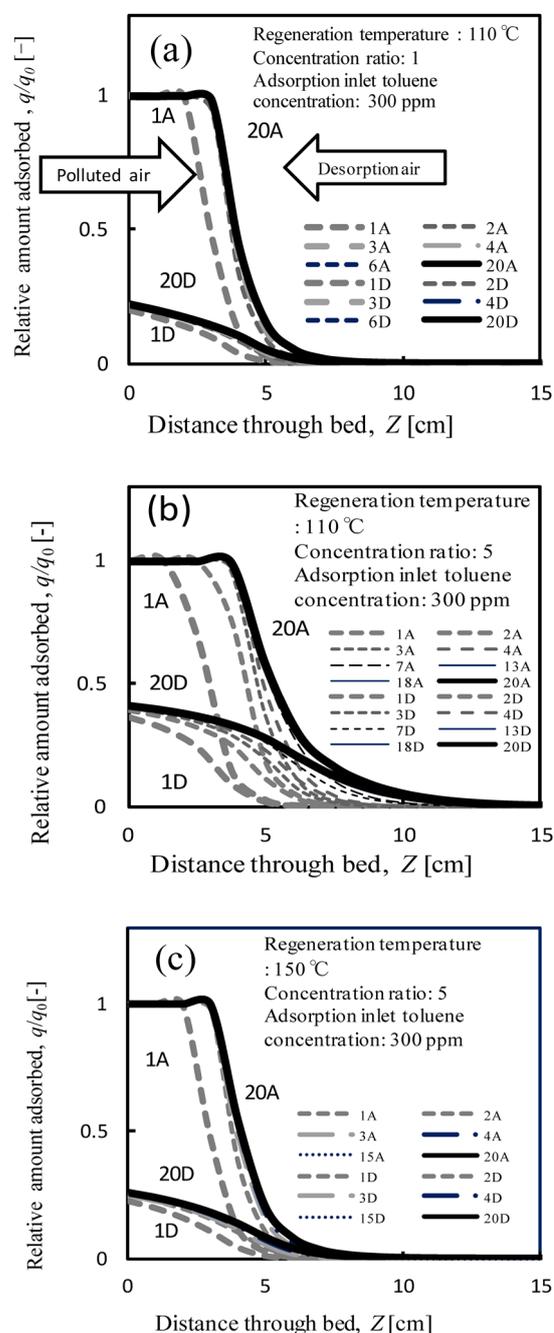
Fig. 12 Progress of the regeneration loading profiles to the cyclic steady-state operation, cycle numbers are indicated on the curves; NA: adsorbent loading profile at the end of adsorption after N cycle times, ND: adsorbent loading profile at the end of desorption after N cycle times, bed length: 15 cm, initial toluene concentration: 300 ppm (a) regeneration temperature: 110°C, concentration ratio: 1 (b) regeneration temperature: 110°C, concentration ratio: 5 (c) regeneration temperature: 150°C, concentration ratio: 5

the adsorbent loading distance increases and the rate of increase becomes sharper. The adsorbent loading distance at a adsorbed phase concentration of $0.0001\,\mathrm{kmol\,kg^{-1}}$ was calculated in the CSS for a two-bed TSA system.

Increasing the regeneration temperature is very effective in reducing the bed length and CSS convergence times,
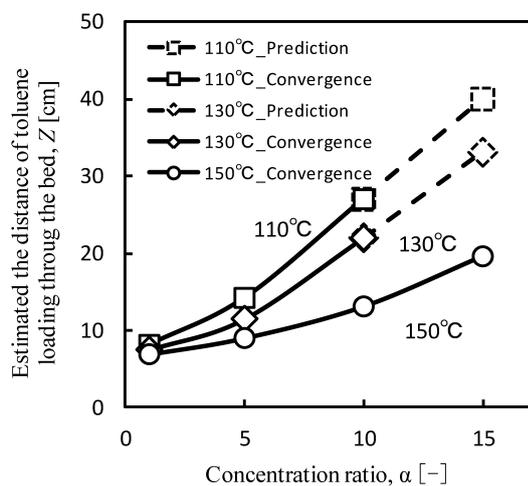
Fig. 13 Effects of concentration ratio and regeneration temperature on distance through bed

particularly in the higher concentration ratio range, but the regeneration temperature may be limited by thermal aging of the adsorbent and the increased cost of higher-grade heat.

Conclusions

An experimental study of desorption has been successfully performed for a low-concentration toluene/nitrogen system using a fixed bed of granular activated carbon. A non-equilibrium, non-adiabatic mathematical model was developed to calculate the desorption concentration curves for desorption runs in a laboratory-scale experimental apparatus.

1. An LDF mass-transfer model with an averaged coefficient was found to provide an acceptable fit to the measured data for desorption tests using a temperature-dependent extended-Langmuir equilibrium equation.

2. A parametric study of this new hybrid system was performed as a function of concentration ratio and exhaust gas temperature for the assumed steady-state condition to assess the effect of concentration time on energy savings. The theoretical study results suggested that supplementary fuel for combustion was not needed, or could be greatly reduced by concentrating VOCs in polluted air in a small amount of purge air. The required concentration ratio was highly affected by the temperature and flow rate of the exhaust gas to the atmosphere.

3. It was verified that the VOCs concentration ratio could be changed by varying the amount of purge air for desorption, in a simulation study of TSA CSS operation.

4. As a result of concentrating the VOCs gas into a small air stream prior to catalytic combustion, auxiliary heat to sustain catalytic combustion was not needed, or could be greatly reduced, and the heat of exhaust gas emitted to the atmosphere was lowered.

5. The results of this study could be used to provide guidance on the development and design of new VOCs treatment processes.

Nomenclature

a_V	=	surface area of particle per unit volume	[$m^2 m^{-3}$]
C	=	gas-phase concentration	[ppm] or [$kmol\,m^{-3}$]
C_{pai}	=	specific heat capacity of adsorbed phase	
			[$MJ\,kmol^{-1}K^{-1}$] or [$MJ\,kg^{-1}K^{-1}$]
C_{pg}	=	specific gas-phase heat capacity	
			[$MJ\,kmol^{-1}K^{-1}$] or [$MJ\,kg^{-1}K^{-1}$]
C_{pgT}	=	mean gas heat capacity at temperature T (25°C basis)	
			[$KJ\,Nm^{-3}K^{-1}$]
C_{ps}	=	specific heat capacity of adsorbent	
			[$MJ\,kmol^{-1}K^{-1}$] or [$MJ\,kg^{-1}K^{-1}$]
C_{pw}	=	specific heat capacity of adsorbed phase	
			[$MJ\,kmol^{-1}K^{-1}$] or [$MJ\,kg^{-1}K^{-1}$]
C_{vg}	=	specific heat capacity of adsorbed phase	
			[$MJ\,kmol^{-1}K^{-1}$] or [$MJ\,kg^{-1}K^{-1}$]
C_0	=	inlet solute concentration	[ppm] or [$kmol\,m^{-3}$]
C^*	=	equilibrium with $\bar{q}$	[ppm] or [$kmol\,m^{-3}$]
D_B	=	bed diameter	[m]
dp	=	particle diameter	[m]
F	=	flow rate	[$m^3 h^{-1}$] or [$Nm^3 h^{-1}$]
FR	=	ratio of flow rate for feed to purge gas	[—]
H_{adi}	=	heat of adsorption of component i	
			[$MJ \cdot kmol^{-1}$] or [$MJ \cdot kg^{-1}$]
H_{air}	=	heat of desorption air for adsorber	[$KJ\,h^{-1}$]
H_{out}	=	heat of exhaust gas to atmosphere	[$KJ\,h^{-1}$]
H_{VOC}	=	combustion heat of VOCs desorbed at adsorber	[$KJ\,h^{-1}$]
h_{amb}	=	wall-ambient heat transfer coefficient	[$MW\,m^{-1}K^{-1}$]
h_s	=	gas–solid heat transfer coefficient	[$MW\,m^{-1}K^{-1}$]
h_w	=	gas–wall heat transfer coefficient	[$MW\,m^{-1}K^{-1}$]
IP_1	=	extended-Langmuir isotherm parameter	[$kmol\,kg^{-1}$]
IP_2	=	extended-Langmuir isotherm parameter	[K]
IP_3	=	extended-Langmuir isotherm parameter	[$kmol\,m^{-3}$]
IP_4	=	extended-Langmuir isotherm parameter	[K]
$K_F a_v$	=	overall mass-transfer coefficient, based on gas-phase concentration	[s^{-1}]
$\overline{K_F a_V}$	=	averaged overall mass-transfer coefficient, based on gas-phase concentration	[s^{-1}]
k_F	=	fluid film mass-transfer coefficient	[$m\,s^{-1}$]
k_g	=	gas phase thermal conductivity	[$MW\,m^{-1}K^{-1}$]
n	=	sample number	[—]
P_r	=	Prandl number ($= \mu C_{pg}/k_g$)	[—]
p	=	pressure	[bar]
Q	=	supplementary heat or surplus heat for sustaining catalytic combustion	[$MJ\,h^{-1}$]
q	=	amount adsorbed	[$kg\,kg^{-1}$] or [$kmol\,kg^{-1}$]
$\bar{q}$	=	averaged amount adsorbed	[$kg\,kg^{-1}$] or [$kmol\,kg^{-1}$]
q^*	=	assumed amount adsorbed in equilibrium with C for Eq. (6)	[$kg\,kg^{-1}$] or [$kmol\,kg^{-1}$]
q_0	=	amount adsorbed in equilibrium with c_0	[$kg\,kg^{-1}$] or [$kmol\,kg^{-1}$]
R	=	gas constant $= (8.314)$	[$J\,mol^{-1}T^{-1}$]
Re_p	=	Reynolds number based on particle diameter ($= d_p u \rho_{pg}/\mu$)	[—]
ST	=	target temperature in sigmoid curve	[°C] or [K]
St	=	time period of sigmoid curve	[s] or [min]

T	=	Celsius or absolute temperature	[°C] or [K]
t	=	time	[s] or [min]
u	=	superficial gas velocity	[m s^{-1}]
W_T	=	width of column wall	[m]
z	=	bed length	[m]
β	=	adsorption coefficient ($= q_0/C_0$)	[m^3 kg^{-1}]
ε	=	void fraction of adsorbent (extra particle)	[—]
μ	=	fluid viscosity	[kg m^{-1} s^{-1}]
ρ	=	density	[kg m^{-3}] or [kmol m^{-3}]

‹Subscripts›

air	=	desorption air for adsorber
amb	=	ambient condition
LDFC	=	estimated by LDFC curve-fitting method
MTZ	=	estimated by MTZ method
g	=	gaseous condition
i	=	component number
out	=	exhaust gas to atmosphere
pair	=	polluted air
s	=	solid condition
w	=	wall condition
0	=	entrance condition

‹Superscripts›

*	=	equilibrium condition
⁻	=	averaged condition

Literature Cited

Aspen Technology, Inc.; Aspen Adsorption 2006 Adsorption Reference Guide, pp. 241–247, Cambridge, U.S.A. (2006)

Basmadjian, D. B., K. D. Ha and C. Y. Pan; "Nonisothermal Desorption by Gas Purge of Single Solutes in Fixed-Bed Adsorbers, I. Equilibrium Theory," *Ind. Eng. Chem. Process Des. Dev.*, **14**, 328–340 (1975)

Chuang, C. L., P. C. Chiang and E. E. Chang; "Modeling VOCs Adsorption onto Activated Carbon," *Chemosphere*, **53**, 17–27 (2003)

Guo, Y., M. Sakurai, H. Kameyama, A. Matsuyama and Y. Kudoh; "Preparation of Alumite Support and Preliminary Activity Investigation for NO Removal in SCR-HC over Alumite Catalyst," *J. Chem. Eng. Japan*, **36**, 1470–1479 (2003)

Huang, C.-C. and J. R. Fair; "Study of the Adsorption and Desorption of Multiple Adsorbates in a Fixed Bed," *AIChE J.*, **34**, 1861–1877 (1988)

Huang, C.-C., T.-I. Hwu and Y.-H. Hsia; "Recovery of Acetone Vapor by a Thermal Swing Adsorber with Activated Carbon," *J. Chem. Eng. Japan*, **26**, 21–27 (1993)

Hwang, K. S., D. K. Choi, S. Y. Gong and S. Y. Cho; "Adsorption and Thermal Regeneration of Methylene Chloride Vapor on an Activated Carbon Bed," *Chem. Eng. Sci.*, **52**, 1111–1123 (1997)

Kameyama, H.; "Alumite Catalysts—The Applications to the Fields of Environment and Energy—" (in Japanese), *Chem. Eng. J.*, **69**, 244–247 (2005)

Kawazoe, K.; "Mass Transfer Mechanism of Adsorption," *Kagaku Kogaku* (*Chem. Eng.*, *Japan*), **29**, 404–409 (1965)

Ko, D., M. Kim, I. Moon and D.-K. Choi; "Analysis of Purge Gas Temperature in Cyclic TSA Process," *Chem. Eng. Sci.*, **57**, 179–195 (2002a)

Ko, D., I. Moon and D.-K. Choi; "Analysis of the Contact Time in a Cyclic Thermal Swing Adsorption Process," *Ind. Eng. Chem. Res.*, **41**, 1603–1615 (2002b)

Kumar, R. and G. R. Dissinger; "Nonequilibrium, Nonisothermal Desorption of Single Adsorbate by Purge," *Ind. Eng. Chem. Process Des. Dev.*, **25**, 456–464 (1986)

Lin, Y. C. and F. T. Chang; "Optimizing Operating Parameters of a Honeycomb Zeolite Rotor Concentrator for Processing TFT-LCD Volatile Organic Compounds with Competitive Adsorption Characteristics," *J. Hazard. Mater.*, **164**, 517–526 (2009)

Malek, A. and S. Farook; "Comparison of Isotherm Models for Hydrocarbon Adsorption on Activated Carbon," *AIChE J.*, **42**, 3191–3201 (1996)

Mitsuma, Y., Y. Ota and T. Hirose; "Performance of Thermal Swing Honeycomb VOC Concentrators," *J. Chem. Eng. Japan*, **31**, 482–484 (1998)

Ruthven, D. M.; Principle of Adsorption and Adsorption Process, pp. 346–351, John Wiley & Sons, New York, U.S.A. (1984)

Schork, J. M. and J. R. Fair; "Parametric Analysis of Thermal Regeneration of Adsorption Beds," *Ind. Eng. Chem. Res.*, **27**, 457–469 (1988)

Ueno, M., T. Yamaguchi, S. Kawada, M. Sakurai and H. Kameyama; "Development of VOCs Concentration/Combustion Process with Adsorbent made from Wood Waste and Electrically Heated Alumite Catalyst," Proc. 72nd Annual Meeting of the Society of Chemical Engineers, Japan, H319, Kagoshima, Japan (2010)

Yamaguchi, T., R. Iuchi, K. Aoki, M. Sakurai and H. Kameyama; "Study of Adsorption System Applying to VOCs Abatement System with Electrically Heated Alumite Catalytic Oxidizer," Proc. 43rd Autumn Meeting of the Society of Chemical Engineers, Japan, J108, Nagoya, Japan (2011)

Yamaguchi, T., R. Iuchi, K. Aoki, M. Sakurai and H. Kameyama; "Parametric Study of Low Concentration Toluene Adsorption on Activated Carbon by MTZ Method and Nonlinear Regression Using LDF Model," *Kagaku Kogaku Ronbunshu*, **39**, 18–27 (2013)

Yun, J.-H., D.-K. Choi and H. Moon; "Benzene Adsorption and Hot Purge Regeneration in Activated Carbon Beds," *Chem. Eng. Sci.*, **55**, 5857–5872 (2000)